JOURNAL OF GEOPHYSICAL RESEARCH, VOL. 98, NO. A8, PAGES 13,557–13,564, AUGUST 1, 1993

Large-Amplitude Auroral Electric Fields Measured With DE 1

D. R. WEIMER

Geophysical Institute, University of Alaska, Fairbanks

D. A. GURNETT

Department of Physics and Astronomy, University of Iowa, Iowa City

A large fraction of the available electric field data from the plasma wave instrument (PWI) on the Dynamics Explorer (DE) 1 satellite has recently been searched for events with large-amplitude (over 100 mV m^{-1}) electric fields. The magnitude and distribution of these peak events as functions of altitude have been determined. The largest amplitudes were found between 1.4 and 2.5 R_E and the probability of finding large electric fields was greatest in the range of 1.5 to 1.7 R_E. However, when the measured electric field values are "mapped" to the Earth's surface in order to account for the geometry of the geomagnetic field lines, then the mapped values always increase with increasing altitude. This radial dependence is considered to be evidence for magnetic field-aligned electric fields. The largest electric field that was detected with the DE 1 instrument had a magnitude exceeding 840 mV m^{-1} and was found at 1.45 R_E. This field appears to be associated with a low-frequency wave, whereas the more commonly observed large-amplitude events have longer durations, are generally found at higher altitudes, and appear to be due to static electric fields. It appears that two types of phenomena are being observed. A study of all electric field measurements, rather than just those with large amplitudes, was also conducted. It was found that at subauroral latitudes the average mapped electric field is nearly constant with altitude, as it should be where there are no magnetic field-aligned potential drops. Small variations can be accounted for by long-term changes in geomagnetic activity. However, within auroral latitudes the average value of the mapped electric field increases as altitude increases. The largest gradients are found between 1.3 and 2 R_E. There is evidence for a "split" potential distribution, with an additional potential drop located above 2.7 R_E.

INTRODUCTION

Electric fields with amplitudes over 100 mV m^{-1} had been reported over 15 years ago by *Mozer et al.* [1977], using measurements from the S3-3 satellite. Subsequently, events with electric field amplitudes as large as 500 mV m^{-1} or greater were also found in these same data [*Mozer et al.*, 1980]. The large electric fields in these events were usually confined to a relatively small region, only several kilometers wide, and often reversed directions to form an oppositely directed pair. These small-scale events are commonly referred to as "electrostatic shocks," and they are usually found on auroral magnetic field lines at altitudes greater than 2000 km. These structures were also linked to auroral arcs [*Torbert and Mozer*, 1978; *Kletzing et al.*, 1983]. In an analysis of the distribution of all shocks detected with the S3-3 satellite, *Bennett et al.* [1983] found that the shocks occur within the auroral oval. The occurrence frequency increased sharply with altitude up to 5000 km, and at a slower rate above 5000 km altitude.

The large-amplitude electric fields in the auroral zone appear to play an important role in auroral particle acceleration, yet the physics of the phenomena are not well understood. The evidence from the S3-3 satellite indicates that these fields are a static, "DC phenomenon" [*Mozer et al.*, 1980]. Electric and magnetic field measurements from Dynamics Explorer (DE) 1 have also been used to show that the characteristics of the large-amplitude electric fields in some cases are consistent with quasi-static, spatial variations of the electric potential, related to magnetic field-aligned currents and potential drops [*Weimer et al.*, 1987]. With data from both the DE 1 and DE 2 satellites near magnetic conjunctions, *Weimer et al.* [1985] found that the large-magnitude electric fields are found at high altitudes but not near the ionosphere and that their amplitude depends upon a spatial scale length.

Field-aligned potential drops have also been inferred from barium release experiments [*Wescott et al.*, 1976]. It is not known exactly how the magnetic field-aligned electric fields are supported in the magnetospheric plasma, although it is generally thought that electric double layers may play a role [*Shawhan et al.*, 1978; *Temerin et al.*, 1981]. Many small double layers and other solitary structures may contribute to the total potential drop along the field lines [*Block and Fälthammar*, 1990].

The topic of field-aligned electric fields is still a subject of considerable controversy. *Haerendel* [1990] considers that the large electric field events are Alfvén waves. *Bryant et al.* [1991] have challenged the evidence for quasi-static, magnetic field-aligned potential drops, in favor of a theory of auroral electron acceleration by wave-particle interaction. Even among those who favor the quasi-static theory, there is not a unanimous agreement as to the use of the term "electrostatic shock" to refer to large-amplitude events.

The large-amplitude electric fields, whatever they may be, appear to play a crucial role in auroral particle acceleration. Large electric fields similar to those detected with S3-3 had been found in the Viking data [*Block et al.*, 1987], but the only comprehensive surveys of this phenomena published to date have used data from just the S3-3 satellite. It is important that a verification be conducted, using data from a different instrument. Also, the apogee of S3-3 was at an altitude of only 8000 km (2.26 R_E) so the distribution of the large-amplitude events above this distance is unknown, other

Paper number 93JA00793.
0148-0227/93/93JA-00793$05.00

than a report of eight events detected with the ISEE 1 satellite between 2.5 and 7 R_E [*Mozer*, 1981].

The DE 1 satellite is ideal for studying the altitude distribution of the large-amplitude electric fields, since its highly elliptical orbit allowed it to sample the range of 1.1 to 4.6 R_E for several years. To carry out this study, a large fraction of the available electric field data from the plasma wave instrument (PWI) on the DE 1 satellite has been searched for events with large-amplitude (greater than 100 mV m^{-1}) electric fields. The magnitude and distribution of these peak events as functions of altitude have been determined. The amplitude of the average electric field has also been investigated as a function of altitude, both within and outside of auroral latitudes. Only the component of the electric field that is perpendicular to the magnetic field is considered here.

MEASUREMENTS

Instrumentation

The Dynamics Explorer spacecraft were launched into polar orbits in August of 1981 for the purpose of investigating auroral and magnetospheric processes. The DE 1 satellite collected data until early 1992, when operations were discontinued. The data used for this particular study consist of all electric field measurements from the plasma wave instrument [*Shawhan et al.*, 1981] taken during the period from September 16, 1981, through June 28, 1984.

The DE 1 satellite was spin-stabilized in a "cartwheel mode," with the spin axis perpendicular to the orbit plane. The spin period was approximately 6 s. Quasi-static electric fields were measured in the spin-orbit plane with one pair of long, wire antennas measuring 200 m from tip to tip. These wires also served a dual role as plasma wave sensors. The inner sections of the wires were insulated, and the outermost 29 m of each element was left uninsulated to serve as probes for measuring the "floating potential" of the plasma.

The electric field is computed using $E=\Delta V/l_{eff}$ [*Fahleson*, 1967; *Cauffman and Gurnett*, 1972], where ΔV is the potential difference between the two probes, and l_{eff} is the effective length. Throughout this paper the effective length is assumed to be the distance between the centers of the uninsulated portions of the antenna, which is l_{eff}=171 m. The voltages differences were obtained via two differential amplifiers with high and low gains. The outputs from both differential amplifiers were sampled at a rate of 16 Hz with an 8-bit analog to digital converter. The high-gain amplifier allowed for measurements of electric field amplitudes up to 54 mV m^{-1} at a resolution of 0.42 mV m^{-1}, and the low-gain amplifier allowed for measurements up to 2000 mV m^{-1} at a more coarse resolution of 17.3 mV m^{-1}.

Peak Events

A search was conducted for all large-amplitude events in the DE 1 PWI electric field data base. This search was done with a computer program that counted all events where the electric field exceeded an amplitude of 100 mV m^{-1}. Only data obtained at locations with invariant latitude between 55° and 85° and at a radial distance less than 4 R_E were searched; the electric field measurements tend to be unreliable at higher altitudes, due to the very low plasma density.

The telemetry data files were blocked into logical records spanning 8 s of time, and it was most convenient to conduct the search on a record-by-record basis. It was also necessary to eliminate the counting of false events due to instrumental, telemetry, or recording media errors. In order to exclude these false events we take advantage of the facts that the electric field antenna was rotating with a 6-s period, which modulates the measured fields, and within the large-amplitude events the electric fields tend to reverse signs. Thus a "real" event was expected to have both large positive and negative values in an 8-s record, whereas erroneous signals usually do not change signs. Therefore, instead of simply searching each data record for the largest value, the electric field magnitude for each record was determined by taking the average of the most positive value and the absolute value of the most negative value. An event was counted as being "large" if this average peak magnitude in the record had a value greater than 100 mV m^{-1}, after subtracting the electric field due to the motion of the satellite through the earth's magnetic field. If this criteria was satisfied then the date, time, magnitude, and location of the event were recorded.

Events with large magnitudes could sometimes span two or more records, but it was desired to count such cases as just one event instead of several, so as to not distort the counting statistics. Therefore events were recorded only if they occurred 32 s or more after the previous event. However, if the second or later record in a group had a magnitude larger than the first, then the larger value was used for that one event.

Using this procedure, a total of 1481 distinct events were counted in 5348.6 hours of data. The largest value recorded was 843 mV m^{-1}. Figure 1 shows a scatter plot which gives the magnitude and radial distance of all events. This plot shows that both the magnitudes and occurrence rate of the large-amplitude events tend to rise and fall between 1.4 and 3.1 R_E. However, due to the nature of the elliptical orbit, the DE 1 satellite spent different amounts of time at different altitudes. Therefore, to obtain a true occurrence rate it is necessary to correct for these time differences. In Figure 2 the data have been grouped into bins according to the radial distance. The top graph in Figure 2 shows the number of hours of data (number of records divided by 450) in each bin. The bin widths are 0.2 R_E in all cases. Obviously there are more data at the higher altitudes, where the satellite was

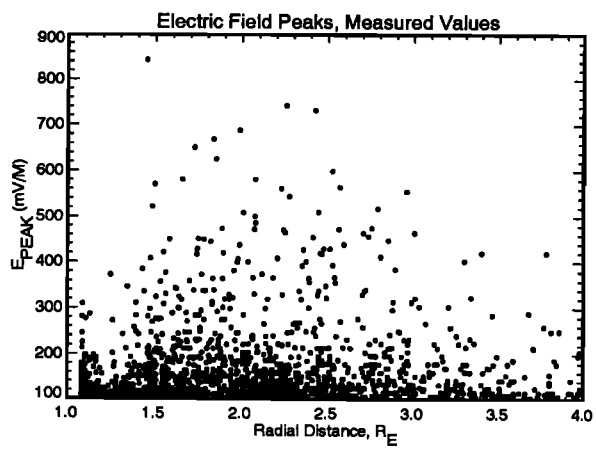

Fig. 1. Electric field peaks, measured values. The amplitudes of all electric fields with amplitudes over 100 mV m^{-1} which were found in the DE 1 data base are shown as a function of radial distance, in units of Earth radii (R_E).

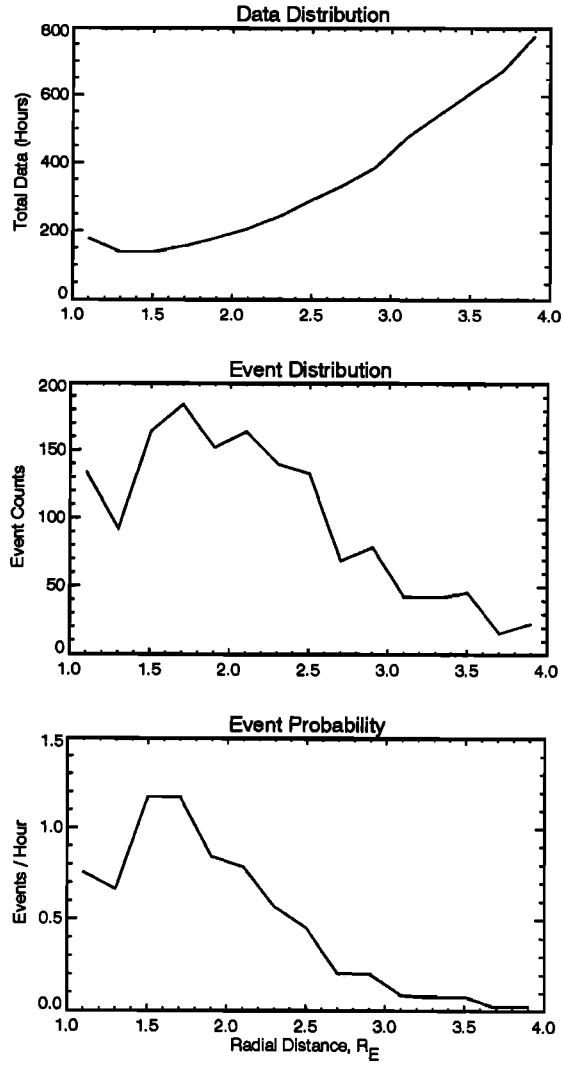

Fig. 2. Large-amplitude electric field occurrence statistics. The top panel shows the number of hours of electric field data in each altitude bin, which are 0.2 R_E wide. The middle panel shows the counts of the large-amplitude electric field events in the same bins, using the same events as are shown in Figure 1. The bottom panel shows the event probability distribution, obtained by dividing the middle graph by the top.

moving much slower. There is also a slight decrease in the amount of data from 1.1 to 1.3 R_E, as the orbit tended to be near the equator and below 55° latitude when it was near 1.3 R_E. The middle panel in Figure 2 shows the number of events counted in each bin, using the same data as shown in Figure 1. The normalized probability of finding an electric field with magnitude over 100 mV m^{-1} is shown in the bottom panel of Figure 2, obtained by dividing the counts by the time interval spent in each bin. There is a very sharp increase in the probability between 1.3 and 1.5 R_E, and a steady decline above 1.7 R_E.

Mapped Values

It is also useful to consider how the "mapped," rather than measured, amplitudes of the large-amplitude electric fields vary with altitude. To review the basic concept of mapping electric field measurements, Figure 3 shows a sketch of two adjacent magnetic field lines labeled *a* and *b*. There are variations of the electric potential in the latitudinal direction (radial at the equator). The potential variations in the azimuthal direction (constant latitude) tend to be much smaller and inconsequential. The electric fields that are perpendicular to the magnetic field at positions r and r' have the following values:

$$E = \frac{\Phi_a - \Phi_b}{dx} \tag{1a}$$

$$E' = \frac{\Phi'_a - \Phi'_b}{dx'} \tag{1b}$$

If there are no magnetic field-aligned potential drops then the potentials are constant along their respective field lines, so that $\Phi'_a=\Phi_a$ and $\Phi'_b=\Phi_b$. Since dx', at the higher altitude, is larger than dx, then the high-altitude electric field has a magnitude less than the electric field at the base of the field line. Given an electric field E' measured at radius r', the mapped electric field E is obtained from

$$E'\left(\frac{dx'}{dx}\right) = E \tag{2}$$

where the ratio dx'/dx is the geometric "mapping factor." For a dipole magnetic field this mapping factor is determined by the L value of the field line (radial distance at the equator) and the radius r':

$$\frac{dx'}{dx} = \left(\frac{4L-3}{4L-3r'}\right)^{1/2} (r')^{3/2} \tag{3}$$

If one now assumes that there is a magnetic field-aligned potential drop $V_{||}$ on field line b, then

$$\Phi'_b = \Phi_b - V_{||} \tag{4}$$

With a substitution of (4) into (1*b*), it can be shown that

$$E'\left(\frac{dx'}{dx}\right) = E + \frac{dV_{||}}{dx} \tag{5}$$

Equation (5) shows that the presence of a gradient in $V_{||}$ will alter the magnitude of the mapped electric field. However, if there is no parallel potential drop, then the mapped electric field will be a constant along the field line. With this in mind, we show in Figure 4 the same data as was graphed in Figure 1, but with the measured values multiplied by the mapping factors which were calculated with (3).

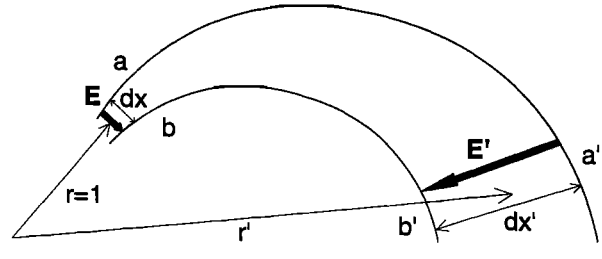

Fig. 3. Illustration of electric field mapping. Electric fields are shown between two adjacent geomagnetic field lines, but at different radial distances. If the magnetic field lines are equipotentials, then the magnitudes of the perpendicular electric fields should vary with altitude, in a manner predictable by the geometry of the dipole field lines. A formula can be used to map the high-altitude measurements to a common reference point, such as 1 R_E.

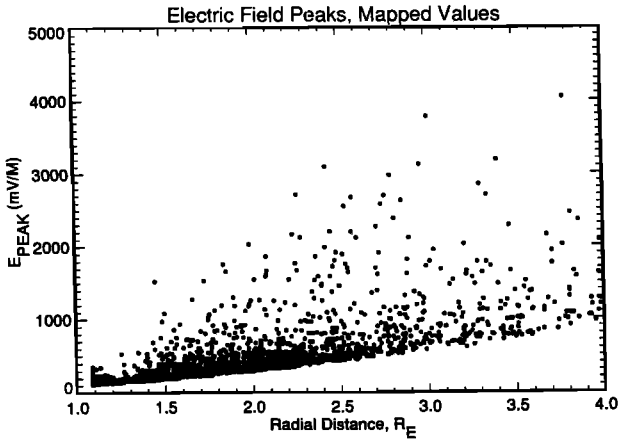

Fig. 4. Electric field peaks, mapped values. The same data that are shown in Figure 1 are graphed, but using the mapped values of the electric field rather than measured values.

Figure 4 confirms that most of the magnetic field-aligned potential drop is located between 1.4 and 1.7 R_E, where the mapped values show their most rapid rise. But whereas the electric field values in Figure 1 tend to rise and then fall as the radial distance (or altitude) increases, the peak values in Figure 4 are always rising. This radial dependence has two implications. First, the fact that the peak mapped values do not reach a level plateau above 1.7 R_E indicates that parallel potential drops still exist above this point. This also implies that the decrease in the measured values above 2.5 R_E, which were shown in Figure 1, are due mostly to the geometrical spreading in the magnetic field lines. This geometrical factor is also responsible for the decreasing probability (above 1.7 R_E) of finding an electric field with a magnitude greater than our arbitrary cut-off value of 100 mV m^{-1}, as shown in Figure 2.

The Largest Event

We next turn our attention to the largest electric field event that was found in this data base. In Figure 1 there is one particularly large datum of 844 mV m^{-1} found at 1.45 R_E. At first glance this one point appears to be due to an instrumental or computer error, but examination of the actual data at high resolution indicates that the measured value is authentic.

This large electric field was detected at 959:30 UT on January 19, 1984, when the satellite was located at an invariant latitude of 66.9° and 2.1 hours magnetic local time. The high-resolution data, obtained from the rotating dipole antenna at 16 samples per second, are shown in the middle panel in Figure 5. This measured electric field has a sinusoidal component due to the satellite's spin. The vertical tic marks at 3-s intervals show the points where the antenna was parallel to the spin-plane component of the geomagnetic field and the spin signal crosses zero. In order to remove the spin modulation the measured electric field values are divided by the sine of the "antenna phase angle," resulting in the graph of the perpendicular electric field shown in the bottom panel in Figure 5. (In order to avoid infinities near the zero crossings, the division is done only where the phase angle is greater than 30°, which results in the periodic gaps in this graph.) By taking the antenna phase angle into consideration, the electric field in this event appears to exceed 1000 mV m^{-1}.

In order to get a picture of the field-aligned current intensity associated with this very large electric field, the top panel of Figure 5 shows the azimuthal or east-west component of the magnetic field measured with the magnetometer on DE 1 [*Farthing et al.*, 1981]. These magnetic field perturbations are also sampled at 16 Hz, and the background geomagnetic field has been subtracted. It is evident from this graph that the large electric field is associated with an intense, upward field-aligned current sheet. The slope of the magnetic field perturbation indicates that the current density was 3.3 μA m^{-2} at the location of the satellite. This current density corresponds to a value of 10.4 μA m^{-2} when mapped to the base of the magnetic field line, which is quite substantial, since values near 1 μA m^{-2} are more typical.

This event is noteworthy not only because of the magnitude of the electric field, but also because of its small temporal/spatial scale. The large electric field, including the reversal, occurred within a time period of 2 s, which corresponds to a width of 15.7 km at a satellite velocity of 7.85 km s^{-1} perpendicular to the magnetic field lines. More importantly, the large electric field is confined within the intense current sheet, and the oppositely directed fields point outward (assuming that the electric fields are perpendicular to the magnetic field; a parallel orientation cannot be ruled out with just one antenna). In contrast, the majority of the large-amplitude electric fields that have been found with DE-1 tend to have a longer duration, are found at higher altitudes, have the upward current sheets embedded within (rather than vice versa), and point inward. As shown by *Weimer et al.* [1987], these more typical events are consistent with the conventional theory of quasi-static, V-shaped auroral potential structures. The different type of electric field that is shown in Figure 5 may perhaps be due to a temporal oscillation at a frequency of about 0.5 Hz. It is noteworthy that the irregular electric field fluctuations increase as the upward current intensity (slope of $B_{E\text{-}W}$) increases. The wavelike nature of these fluctuations, and the fact that they seem to be found only at the low end of the DE 1 orbit, agree with the findings of *Block and Fälthammar* [1990], using data from the Viking satellite. *Block and Fälthammar* [1990, p. 5877] suggest that the electric field fluctuations "below 1 Hz may be due to standing waves trapped within a region of high Alfvén velocity in the altitude range between about a half and a few Earth radii."

Average Values

So far our discussion has been concerned only with the distribution of electric fields with very large magnitudes. Next we consider the trends that are shown by an averaging of all electric field measurements, including values less than 100 mV m^{-1}. The top graph Figure 6 shows the distribution of the data, in total hours per bin, similar to that in Figure 2. There are two lines in each of the graphs in Figure 6; the solid line corresponds to data obtained at an invariant latitude between 65° and 85°, while the dotted line corresponds to data obtained at an invariant latitude in the range of 55° to 65°. The middle graph shows the average of the electric field measured within each altitude bin. These values are always decreasing, for both the low- and high-latitude groups. However, a different picture emerges in the bottom graph, which shows the averages of the mapped electric fields. At the low, subauroral latitudes (dotted line) the mapped values are nearly constant, which would be expected if there are no

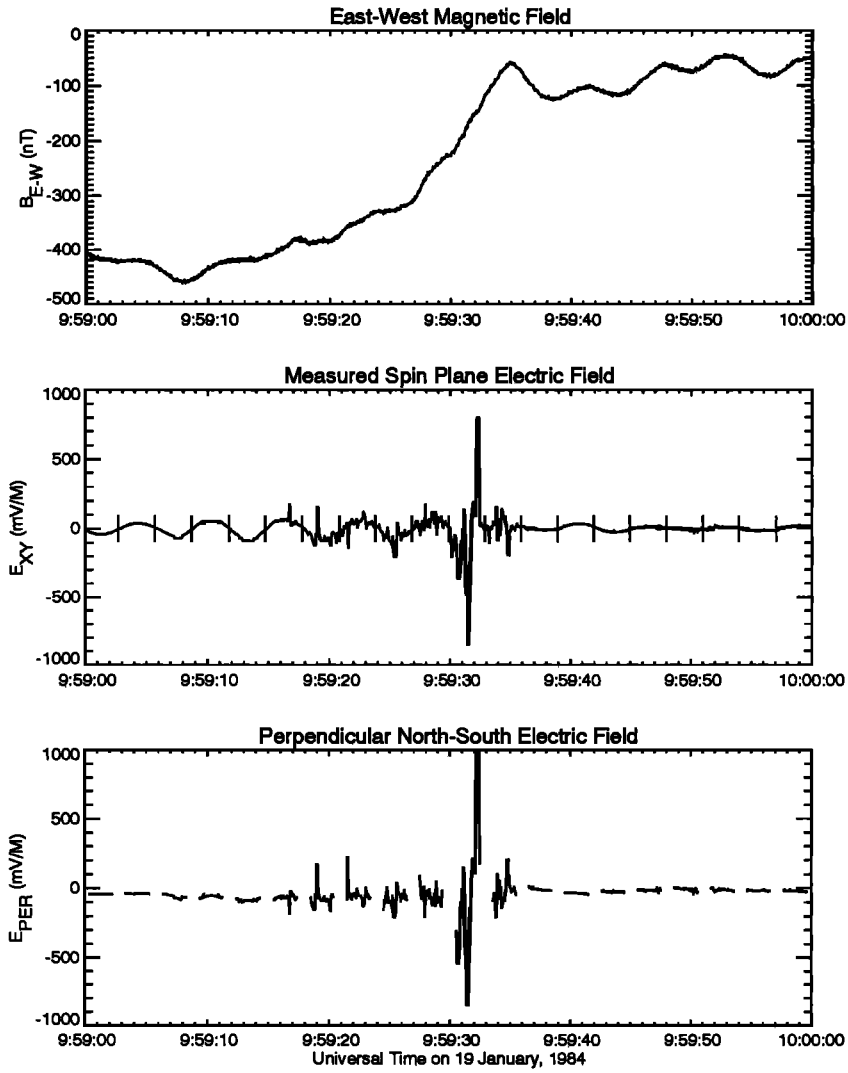

Fig. 5. The event with the largest magnitude measured with DE 1. This electric field, with magnitude exceeding 840 mV m^{-1}, was measured at 0959-1000 UT on January 19, 1984. The middle panel shows the values from the rotating dipole antenna. The vertical tic marks show the points where the antenna is parallel to the magnetic field in the satellite's spin plane. The bottom panel shows the electric field with the spin modulation removed, assuming an orientation perpendicular to the magnetic field. For reference, the top panel shows the perturbations to the azimuthal magnetic field measured simultaneously with the magnetometer on DE 1. A positive slope indicates an upward current, which is relatively intense in this case.

parallel potential drops. However, at the high, auroral latitudes (solid line) the mapped electric field increases as altitude increases.

It is peculiar that, after an initial increase around 1.5 R_E, the mapped electric field reaches a level plateau and then increases again above 2.7 R_E. This plateau could possibly be an instrumental effect, as the plasma wave instrument's antennas on DE 1 were not optimized for measurements of static electric fields in the very low plasma densities which are encountered at high altitudes. However, this seems unlikely, as the mapped electric field at subauroral latitudes would show a similar instrumental bias, which is not the case.

It was also suspected that long-term variations in geomagnetic activity might be the cause of apparent changes in the average electric field as a function of altitude. The highly elliptical orbit of DE 1 had apsidal motion (with perigee moving between the poles and equator) such that the majority of the data at the mid-altitude range were obtained at time periods different from when the data were obtained at lower and higher altitudes. More intense electric fields could have been formed when (and where) the geomagnetic activity was higher.

We have conducted an analysis of the Auroral Electrojet (*AE*) indices that were measured concurrently with these DE 1 data in order to detect such a bias due to long-term changes in geomagnetic activity. The results are shown in Figure 7, which shows the average *AE* index as a function of the satellite's radial distance, for both the auroral (solid line) and subauroral (dotted line) latitudes. When compared to the mapped electric fields that are shown in the bottom of Figure 6, we see that all of the small deviations of the subauroral electric field (dotted line) can be accounted for by the changes in geomagnetic activity. This correlation helps to validate our measurement and mapping process. However, the changes in the mapped electric field within the auroral latitudes (solid line) do not correlate with the geomagnetic activity. Thus the indicated changes in the electric field as a function of radial distance appear to be real.

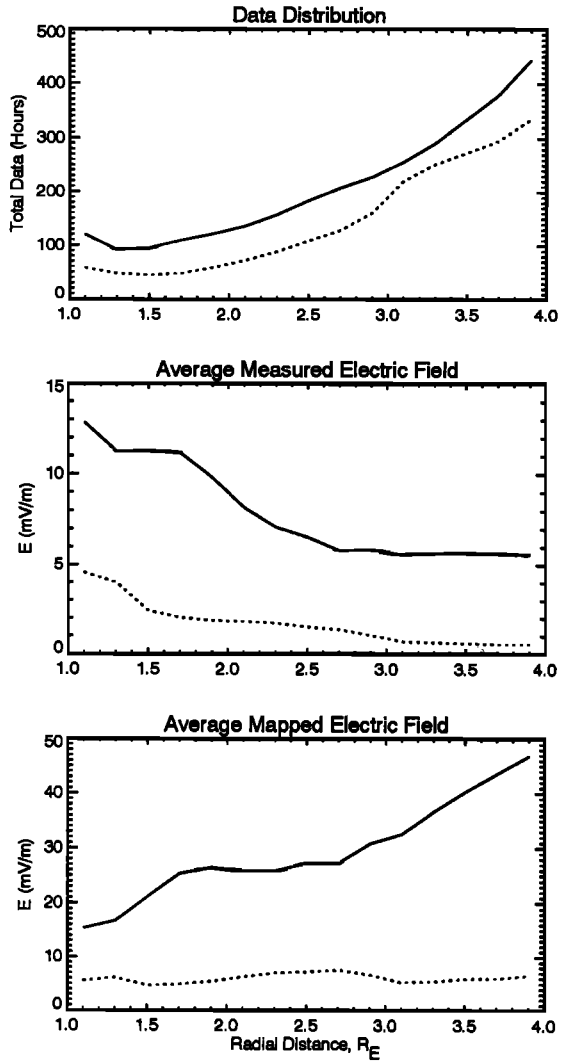

Fig. 6. Average electric fields as functions of radial distance. Every electric field measurement in the data base has been summed and averaged in bins 0.2 R_E wide, for two different latitude ranges. The top panel shows the total hours of data in each bin, for auroral zone data, 65° to 85° invariant latitude (solid line), and subauroral latitudes, 55° to 65° (dotted line). The middle panel shows the averages of the measured electric field values vs. distance, which the bottom panel shows the averages of the mapped electric field values for both latitude ranges.

There is one additional factor that could influence the results that are shown in the bottom of Figure 6. As the local time of the satellite's orbit plane was gradually changing, these data were obtained at various, uneven combinations of local time and altitude. As the largest electric fields are known to be found within the evening sector [*Bennett et al.*, 1983], this uneven sampling could perhaps bias these results. In fact, separation of the data by local time shows that most of the measurements that were obtained within auroral latitudes at 1.5 R_E were on the dusk side ($MLT > 12$ hour), while at 2.5 R_E the measurements were predominately on the dawn side ($MLT < 12$ hour). However, the variations in the mapped electric field as a function of altitude are approximately the same on both sides, with similar plateaus between 2.0 and 2.5 R_E.

Effect of Capacitive Coupling

It should be pointed out that the peak electric field could, under some circumstances, be even larger than the values

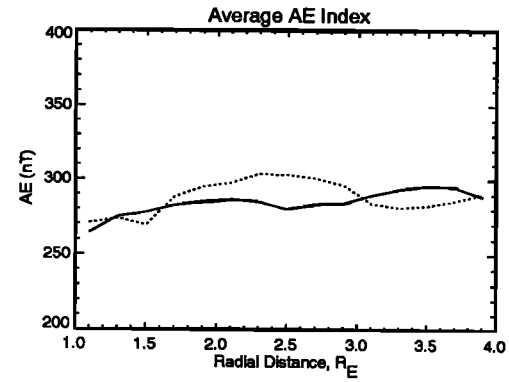

Fig. 7. Average auroral electrojet index as a function of radial distance. Although these indices are measured on the ground, this graph shows how the geomagnetic activity varied while DE 1 sampled the electric fields at different altitudes. The solid line shows the variations while DE 1 was within the auroral zone, and the dotted line shows the changes while the satellite was at subauroral latitudes.

quoted in this paper. Our calculation of the electric field assumes that the DE 1 antenna is resistively coupled to the plasma through the uninsulated tips of the antenna. For rapidly varying fields, such as occur during the spiky events, a significant capacitive coupling may also occur. Since capacitive coupling occurs equally well through both the insulated and uninsulated portions of the antenna, the net effect is to reduce the effective length of the antenna. In the case of purely capacitive coupling, as is often assumed for plasma wave studies, the effective length is one-half of the tip-to-tip length, which for DE 1 is $l_{eff}(C)$=100 m. Since the effective length for purely resistive coupling is $l_{eff}(R)$=171 m, if purely capacitive coupling dominates then the peak electric fields would be increased by a factor of 1.7. The relatively simple circuit model shown in Figure 8 can be used to evaluate the transition from resistive to capacitive coupling. In this model, C is the sheath capacitance and R is the sheath resistance. For large Debye lengths the sheath capacity is approximately the free space value, which for a long thin wire

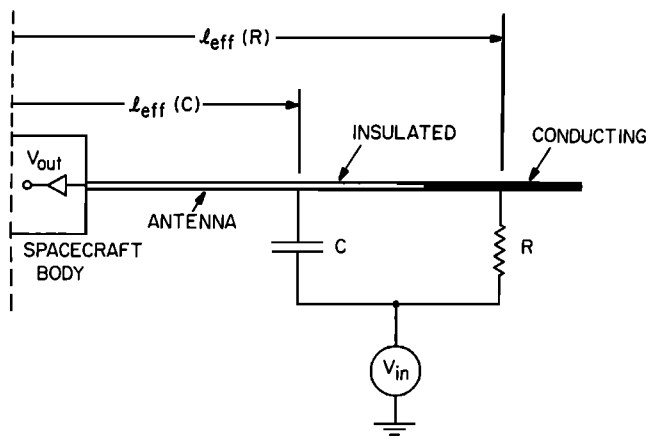

Fig. 8. Illustration of effective antenna lengths. The thin-wire antennas on the DE 1 plasma wave instrument have an insulated section towards the spacecraft and an outer, conducting section. The plasma sheath around the antenna has a capacitance C and resistance R while V_{in} represents the plasma's floating potential. At low frequencies the coupling between the plasma and antenna is resistive, while at high frequencies the coupling is capacitive. The result is that the effective length of the antenna, l_{eff}, depends on frequency.

is approximately

$$C = \frac{2\pi\varepsilon_0 L}{\ln\left(\frac{L}{a}\right) - 1} \quad (6)$$

where ε_0 is the permittivity of free space, L=100 m is the element length, and a=0.02 cm is the radius of the wire. Using the nominal values, the capacitance works out to be C=450 pf. The sheath resistance is more difficult to estimate, since it depends on the plasma density and various other parameters. Generally, the sheath resistance increases as the plasma density decreases. For plasma densities less than 1 cm^{-3}, which often occurs at high altitudes, the sheath resistance is known to be nearly comparable to the preamplifier input impedance (~ 10^{10} ohm). It is easy to show that the transition from resistive to capacitive coupling occurs at a frequency $\omega_c = 1/RC$. Using the antenna capacity estimated above, and a resistance of 10^9 ohm, which is representative of the plasma densities encountered near apogee, the transition frequency is $\omega_c \approx 2$ Hz. Thus, near apogee, it is likely that short, spiky signals occurring on time scales of a fraction of a second are capacitively coupled to the antenna, which would increase the field strengths by as much as a factor of 1.7. We note that for spherical probes, such as were flown on S3-3, the transition frequency is expected to be higher (since C is smaller), so there is a lower probability of underestimating the electric field magnitude.

CONCLUSIONS

The results of this survey of the DE 1 electric field data confirm the earlier discovery with the S3-3 satellite of large-amplitude auroral electric fields [*Mozer et al.*, 1977]. The data from the S3-3 satellite had indicated that the occurrence of "electrostatic shocks" was always increasing, up to the high-altitude limit of the satellite's orbit at 2.26 R_E; the higher orbit of DE 1 has enabled this study of the distribution of large-amplitude electric fields up to 4 R_E. After taking into account the time spent by the DE 1 satellite at different altitudes, it has been found that the probability of detecting electric fields greater than 100 mV m^{-1} peaks between 1.4 and 1.8 R_E, with a steadily decreasing probability at higher altitudes. Previously it had seemed as if the DE 1 measurements were in disagreement with the S3-3 observations, as the large electric fields did not appear in the data as frequently. The results of this survey show that this apparent disagreement was due to the fact that electric fields with large amplitudes are found with the highest probability at the altitude range where S3-3 spent the most amount of time and DE 1 spent the least amount of time. When this is taken into consideration, there is no disagreement. Also, the high-frequency nature of these events may cause the plasma-antenna coupling on DE 1 to be capacitive rather than resistive, which causes an under-estimate of the amplitude. Another factor is the fact that DE 1 has only one rotating antenna, which reduces the chances of measuring the peak electric field value.

The peak magnitudes of the electric fields tend to rise and then fall as altitude increases. However, if the geometrical spreading of the geomagnetic field lines is taken into consideration, then the mapped values always increase with increasing altitude. It has also been informative to examine how the average of all electric field measurements, rather than just the peak events, changes with altitude. Whereas the average measured electric field decreases with increasing altitude, the mapped electric field increases within the auroral zone and holds steady at lower latitudes. The data indicates that the magnetic field-aligned potential drops, which cause the perpendicular electric fields to increase, are located mainly between 1.3 and 2 R_E. There is also evidence of additional potential drops above 2.7 R_E. A split in the distribution of the field-aligned potential drops would be consistent with the findings of *Gurgiolo and Burch* [1988], using measurements of electron distribution functions from DE 1.

The largest electric field detected with DE 1 had a measured magnitude of 840 mV m^{-1}; with the probe antenna's angle with respect to the magnetic field taken into consideration, the peak magnitude may have exceeded 1000 mV m^{-1}. However, there were some major differences between this event and the more typical patterns which were detected with DE 1, indicating that it might have been due to a plasma wave rather than an electrostatic structure. There appear to be two types of large-amplitude electric field events. Hence we hesitate to apply a more descriptive term to the class as a whole. Perhaps the wavelike structures are found at lower altitudes, within the field-aligned potential drops, while the wider, quasi-static structures are found at higher altitudes, above the potential drops. Further electric field measurements from the upcoming FAST and Polar missions will undoubtfully help in the understanding of these large-amplitude auroral electric fields.

Acknowledgments. This paper is dedicated to the memory of Stan Shawhan, who first proposed this survey in 1981 after the launch of the Dynamics Explorer satellites, but before the data were available. The authors thank Jim Slavin for providing the DE 1 magnetometer data. D.R.W. thanks Bob Hoffman for funding this research through NASA grant NAG5-1780 to the University of Alaska.

The Editor thanks L. P. Block and F. S. Mozer for their assistance in evaluating this paper.

REFERENCES

Bennett, E. L., M. Temerin and F. S. Mozer, The distribution of auroral electrostatic shocks below 8000 km altitude, *J. Geophys. Res., 89,* 7107-7120, 1983.

Block, L. P., and C.-G. Fälthammar, The role of magnetic-field-aligned electric fields in auroral acceleration, *J. Geophys. Res., 95,* 5877-5888, 1990.

Block, L. P., C.-G. Fälthammar, P.-A. Lindqvist, G. Marklund, F. S. Mozer, A. Pedersen, T. A. Potemra, and L. J. Zanetti, Electric field measurements on Viking: First results, *Geophys. Res. Lett., 14,* 435-438, 1987.

Bryant, D. A., A. C. Cook, Z.-S. Wang, U. de Angelis, and C. H. Perry, *J. Geophys. Res., 96,* 13,829-13,839, 1991.

Cauffman, D. P., and D. A. Gurnett, Satellite measurements of high latitude convection electric fields, *Space Sci. Rev., 13,* 369-410, 1972.

Farthing, W. H., M. Sugiura, B. G. Ledley, and L. J. Cahill, Magnetic field observations on DE A and B, *Space Sci. Instrum., 5,* 551-560, 1981.

Fahleson, U., Theory of electric field measurements conducted in the magnetosphere with electric probes, *Space Sci. Rev., 7,* 238-262, 1967.

Gurgiolo, C., and J. L. Burch, Simulation of electron distributions within auroral acceleration regions, *J. Geophys. Res., 93,* 3989-4003, 1988.

Haerendel, G., Field-aligned currents in the earth's magnetosphere, in *Physics of Magnetic Flux Ropes, Geophys. Monogr. Series,* vol. 58, edited by C. T. Russell, E. R. Priest, and L. C. Lee, pp. 539-553, AGU, Washington, D. C., 1990.

Kletzing, C., C. Cattell, F. S. Mozer, S.-I. Akasofu, and K. Makita, Evidence for electrostatic shocks as the source of discrete auroral arcs, *J. Geophys. Res., 88,* 4105-4113, 1983.

Mozer, F. S., C. W. Carlson, M. K. Hudson, R. B. Torbert, B. Parady, J. Yatteau, and M. C. Kelley, Observations of paired electrostatic shocks in the polar magnetosphere, *Phys. Rev. Lett., 38,* 292-295, 1977.

Mozer, F. S., C. A. Cattell, M. K. Hudson, R. L. Lysak, M. Temerin, and R. B. Torbert, Satellite measurements and theories of low altitude auroral particle acceleration, *Space Sci. Rev., 27,* 155-213, 1980.

Mozer, F. S., ISEE-1 observations of electrostatic shocks on auroral zone field lines between 2.5 and 7 Earth radii, *Geophys. Res. Lett., 8,* 823-826, 1981.

Shawhan, S. D., C.-G. Fälthammar, and L. P. Block, On the nature of large auroral zone electric fields at 1-R_E altitude, *J. Geophys. Res., 83,* 1049-1054, 1978.

Shawhan, S. D., D. A. Gurnett, D. Odem, R. A. Helliwell, and C. G. Park, The plasma wave and quasi-static electric field instrument (PWI) for Dynamics Explorer-A, *Space Sci. Instrum., 5,* 535-550, 1981.

Temerin, M., C. Cattell, R. Lysak, M. Hudson, R. B. Torbert, F. S. Mozer, R. D. Sharp, and P. M. Kitner, The small-scale structure of electrostatic shocks, *J. Geophys. Res., 86,* 11,278-11,298, 1981.

Torbert, R. B., and F. S. Mozer, Electrostatic shocks as the source of discrete auroral arcs, *Geophys. Res. Lett., 5,* 135-138, 1978.

Weimer, D. R., C. K. Goertz, D. A. Gurnett, N. C. Maynard, and J. L. Burch, Auroral zone electric fields from DE 1 and 2 at magnetic conjunctions, *J. Geophys. Res., 90,* 7479-7494, 1985.

Weimer, D. R., D. A. Gurnett, C. K. Goertz, J. D. Menietti, J. L. Burch, and M. Sugiura, *J. Geophys. Res., 92,* 187-194, 1987.

Wescott, E. M., H. C. Stenbaek-Nielsen, T. J. Hallinan, T. N. Davis, and H. M. Peek, The Skylab barium plasma injection experiments, 2, Evidence for a double layer, *J. Geophys. Res., 81,* 4495-4502, 1976.

D. A. Gurnett, Department of Physics and Astronomy, University of Iowa, Iowa City, IA 52242.

D. R. Weimer, Geophysical Institute, University of Alaska, Fairbanks, AK 99775-0800.

(Received January 25, 1993;
revised March 18, 1993;
accepted March 19, 1993.)